Infectious Disease Modelling 9 (2024) 10–26

Contents lists available at ScienceDirect

Infectious Disease Modelling

journal homepage: www.keaipublishing.com/idm

Optimal therapy for HIV infection containment and virions inhibition

Paolo Di Giamberardino , Daniela Iacoviello *, Muhammad Zubair

Dept. of Computer, Control and Management Engineering, Sapienza, University of Rome, Via Ariosto 25, 00185, Rome, Italy

ARTICLE INFO

Article history:
Received 1 September 2023
Received in revised form 6 November 2023
Accepted 10 November 2023
Available online 14 November 2023
Handling Editor: Dr Daihai He

Keywords:
Epidemic modeling
HIV-AIDS
Optimal control

ABSTRACT

Prevention and early diagnosis are the best and most effective ways for defeating HIV. There is still no vaccine, but treatments with antiretroviral drugs are now available which, in many cases, allow the infection to become chronic. However, research has highlighted side effects of these drugs and the fact that a flare-up of the infection occurs if the therapy is stopped. In recent years, the presence of virus reserves located in various parts of the body, including the brain, has been hypothesized. The possibility of controlling the infection of healthy cells and of interrupting the proliferation of virions inside the brain has been studied, proposing optimal control strategies.

1. Introduction

Despite undeniable progress in tackling Human Immunodeficiency Virus (HIV), many thousands of deaths are still recorded nowadays, approximately 650.000 in 2021, (WHO).

The HIV is classified into two main types, HIV-1 and HIV-2, with the latter most confined to West Africa and less contagious; in literature and in the following, when referring to HIV generally the most severe one HIV-1 is dealt with.

The comforting aspect is that the number of diagnoses is decreasing, almost halving in the last 25 years; unfortunately, access to treatment still concerns only 75% of the total number of people with a positive diagnosis. A delayed positive diagnosis has two main consequences: the subject could unconsciously infect other people and the start of therapy is delayed. So, besides an effective vaccination, still not available, at least the virus spread could be interrupted by prevention and early diagnosis that have still a fundamental role, (Di Giamberardino et al., 2019), (Deeks et al., 2015), (Di Giamberardino and Iacoviello, 2023), (Di et al., 2020, pp. 197–249). The therapy consists in the treatment with Highly Active Anti-Retroviral Therapy (HAART); in this way HIV can become a manageable chronic health condition, (Eggleton & Nagalli, 2023), even if with possible side effects, (Montessori et al., 2004), (Thapa & Shrestha, 2023). At population level, different control actions can be proposed as strategies for medical intervention at different stages of infection progression (Di et al., 2018a), (Di et al., 2018b).

By means of these therapeutic approaches, the number of infected patients living with HIV is increasing, due to the inhibition of virus replication. Nevertheless, it has been observed that after the suspension of the therapy there is an increase of

* Corresponding author.
E-mail address: daniela.iacoviello@uniroma1.it (D. Iacoviello).
Peer review under responsibility of KeAi Communications Co., Ltd.

https://doi.org/10.1016/j.idm.2023.11.006

the infection, (Levy, 1995); as recalled in (Huang et al., 2017), one reason could be the capability of the residual viremia (a common feature among patients treated with HAART) to lead to cycles of viral replication. This hypothesis was rejected for the lack of new resistance mutations; therefore, it has been argued that HIV is able to persist in viral reservoirs, as the brain, the liver and the gut, (Huang et al., 2017), (Barker & Vaidya, 2020), (Kruize & Kootstra, 2019), (Chen et al., 2022), (Busman-et al., 2021), (Astorga-Gamaza & Buzon, 2021). In (Huang et al., 2017) it is proposed a model in which the variations of the number of CD4+T cells, of the infected and chronically infected cells and the viral load are studied in the tissue, the blood, the testis and the brain, including the mutual influence. Among the virus reservoirs, the brain plays a central role due to experience of many patients of neurocognitive disorders (HAND), with dementia and encephalitis, as if the virus is not stuck in the brain but can move up to the peripheral zones of the body by means of leukocyte. Complicating the fight against HIV is the phenomenon that in (Osborne et al., 2020) is called the *paradox of the blood brain barrier* (BBB): it reduces the effectiveness of medical treatments blocking the crossing inside of drugs, thus representing an obstacle for healing; nevertheless, immune cells can be infected by HIV becoming able to cross the blood−brain−barrier and to form a reservoir allowing the replication of the virus. In (Clifford & Ances, 2013), it has been stressed that the macrophages, cells of the innate immune system, could be infected themselves; if infected they can damage the central nervous system (leading to death); moreover, they can hide the virus to treatments and antibodies, acting as trojan horse. The mechanism of the macrophages infection by HIV is still unclear, as admitted in (Dupont & Sattentau, 2020) where the proposed mechanisms are the phagocytosis, the fusion and nanotubes. In (Lutgen et al., 2020) it is recalled that HIV infects the brain in acute disease, approximately two weeks from the infections; the delay with which HIV is detected implies that generally when the first symptoms appear, the brain can be already involved.

By using compartmental modeling it is possible to study the evolution of the number of healthy cells, of virions and macrophages; in (Barker & Vaidya, 2020) it is proposed an 8-dimension compartmental model distinguishing healthy CD4+T cells and macrophages, inside and outside the brain, and the corresponding infected ones; moreover the virions inside and outside the brain are introduced. The infection occurs by the virions that, what is more dangerous, are fed by the infected cells; this action is discussed in (Barker & Vaidya, 2020) considering an on-off situation, without the introduction of control actions.

In this paper, starting from the cited model (Barker & Vaidya, 2020), four control actions are introduced, aiming at reducing the possibilities of infection and the production of new virions. The control of the infection inside the brain is considered, being aware that, as already mentioned, some pharmacological treatment could not be totally effective against the infected cells located inside the brain.

The paper is organized as follows. In Subsection 2.1 the model proposed in (Barker & Vaidya, 2020) is recalled introducing the control actions; after assessing existence results of the solution, the model is analysed determining the disease free equilibrium. Its stability analysis, discussed in Subsection 3.3, yields the condition for the asymptotic stability of the disease free conditions; moreover, the basic reproduction number is determined. The optimal choice for the control actions, aiming at reducing the number of infected cells avoiding the production of new ones, is introduced in Section 4. Numerical results are proposed and discussed in Section 5; conclusions and further developments are outlined in Section 6.

2. Materials and methods

The mathematical model used in this study is proposed in a recent work (Barker & Vaidya, 2020), in which data from HIV-1 infected macaques were examined. The modelling is implemented at cellular level with a partition of the population distinguishing among the cells outside and inside the brain (the latter indicated with subscript B), and the cells uninfected and infected (the latter identified with superscript $*$); moreover, the virions inside and outside the brain are introduced, V and V_B, respectively. Therefore, the population has 8 categories of cells interacting, as will be described in the next Subsection 2.1.

2.1. Mathematical modeling

To describe the HIV-1 infection in the brain as proposed in (Barker & Vaidya, 2020), the population of cells is partitioned as follows:

- $T(t)$ is the concentration of the uninfected $CD4^+$ T cells at time t;
- $T^*(t)$ is the concentration of the infected $CD4^+$ T cells at time t;
- $M(t)$ is the concentration of the uninfected macrophages in the plasma at time t;
- $M^*(t)$ is the concentration of the infected macrophages in the plasma at time t;
- $M_B(t)$ is the concentration of the uninfected macrophages inside the brain at time t;
- $M_B^*(t)$ is the concentration of the infected macrophages inside the brain at time t;
- $V(t)$ is the concentration of free HIV-1 virions at time t;
- $V_B(t)$ is the concentration of free HIV-1 virions in the brain at time t.

Where concentrations are measured as cells per μl.

The mechanism of the infection is complex. A virion V can infect the CD4+T cells and the macrophages M outside the brain, yielding T^* and M^* respectively; the latter can enter the brain thus increasing M_B^*. Infected T^*, M^* and M_B^* can feed the virions inside and outside the brain in a vicious circle. The rates at which virions V infect T and M cells are β and β_M respectively. Similar dynamics occurs inside the brain, involving the macrophages M_B that could be infected by the virions V_B, with the same rate β_M, thus becoming M_B^*. Only macrophages can cross the brain border; healthy cells M flow into the brain at the rate φ and vice versa, from M_B to M, at the rate ψ; the same holds for the infected cells, with M^* that can transfer from outside to inside the brain M_B^* at the same rate φ, and vice versa, with the rate ψ. Actually, the brain border cross is possible only for macrophages cells at immature growth status, (Kumar et al., 2014), (Prinz & Priller, 2014), but in the present paper, following also (Barker & Vaidya, 2020), the natural cell growth dynamics is not considered. In a more detailed model, with the introduction of these characterization, additional time constants and delays would appear, mainly changing the times but affecting the amplitudes only marginally.

The infected T^* and macrophages cells M^* produce free virions V at the rate p and p_M respectively, as well as, in the brain, the M_B^* cells produce virions V_B at the rate p_M.

Death rates d and δ are defined for the T and T^* cells respectively; d_M is the death rate of the uninfected macrophages outside and inside the brain, as well as the infected macrophages M^* and M_B^* that die at rate δ_M. For the virions V and V_B the death rate is indicated by c. The uninfected T cells and macrophages M are generated at a constant rate of τ and τ_M cells/μL per day respectively.

In (Barker & Vaidya, 2020), it is proposed the introduction of the highly active antiretroviral therapy, simulating that the viral production could be completely removed outside the brain but not effective at all inside. In this paper, a higher number of control actions are introduced aiming at limiting the infection outside (with a control u_1) and inside the brain (with a control u_2), reducing the contact rate β and β_M. Moreover, also the possibility of generation of virions V from the infected cells T^* and M^* is reduced by means of a control u_3 and the generations of virions V_B from cells M_B^* is controlled by limiting the generation rate p_M by means of the control u_4.

Therefore, the infection evolution with control actions can be represented by the following equations:

$$
\begin{aligned}
\dot{T} &= \tau - \beta(1-u_1)VT - dT \\
\dot{T}^* &= \beta(1-u_1)VT - \delta T^* \\
\dot{M} &= \tau_M + \psi M_B - \beta_M(1-u_1)VM - \varphi M - d_M M \\
\dot{M}^* &= \beta_M(1-u_1)VM + \psi M_B^* - \varphi M^* - \delta_M M^* \\
\dot{M}_B &= \varphi M - \psi M_B - \beta_M(1-u_2)V_B M_B - d_M M_B \\
\dot{M}_B^* &= \beta_M(1-u_2)V_B M_B - \psi M_B^* + \varphi M^* - \delta_M M_B^* \\
\dot{V} &= p(1-u_3)T^* + p_M(1-u_3)M^* - cV \\
\dot{V}_B &= p_M(1-u_4)M_B^* - cV_B
\end{aligned}
\tag{1}
$$

whose scheme is shown in Fig. 1.

The amplitude of the controls u_i, $i = 1, \ldots, 4$ can be interpreted as the intensity of efficacy of a treatment and are assumed between 0, meaning no action/effectiveness, and 1, the maximum of the possible effectiveness with a total inhibition of virus propagation.

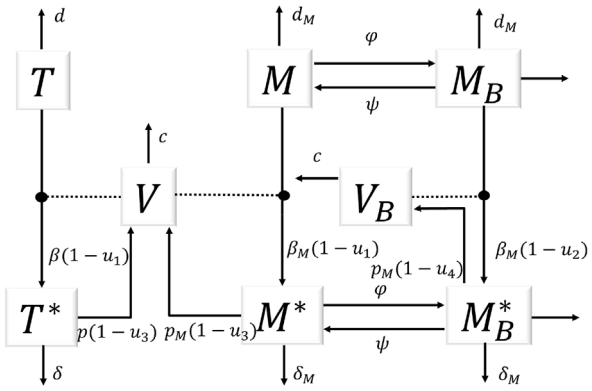

Fig. 1. Block diagram of the controlled proposed model.

The controls have been introduced modelling the known medical actions which aim at reducing the infection as well as the virus replication. A biological description of the mechanisms at the bases of the infection progression and the pharmacological ways of interrupt it are beyond the scope of the present discussion. However, their introduction follows the main lines of actions of the available mechanisms infection inhibition.

Without referring to specific drugs or active principles, according to literature, as in (Zephyr et al., 2021), (Ahemd et al., 2021) and (Agosto et al., 2014), there are different mechanisms known to the authors for the virus fight and the infection containment. One is represented by the *Reverse Transcriptase Inhibitors*, antiretroviral drugs that inhibit activity of viral DNA polymerase required for retrovirus replication, acting on the DNA chain construction and then limiting the virus replication. Such an effect can be produced by nucleoside or nucleotide analog reverse transcriptase inhibitors: this process is called also as chain termination since the nucleosides or nucleotides used have the same structure of the normal ones but they terminate in such a way that no more nucleotides can be added to the DNA chain: the enzyme reverse transcriptase recognizes them as regular and inserts them into the newly synthesized DNA chain which then becomes inactive. Also non-nucleoside reverse transcriptase inhibitors can be used, always leading to damages in the DNA chain construction but through a distortion of the position of the DNA binding sites in the enzyme. Another action is represented by the *Protease Inhibitors*, a class of medications that act by interfering with enzymes that cleave proteins, blocking the development of protein precursors for the production of infectious viral particles.

A different type of intervention is represented by the *Fusion Inhibitors*, able to suppress HIV in the body; HIV needs to enter human host cells to replicate and this is performed binding to their surface and then fusing itself with cell to get inside: fusion inhibitors block this step in the process, preventing HIV from infecting the cells and, then, from replicating. Finally, there are the *Integrase Inhibitors*, a class of antiretroviral drug designed to block the action of integrase, a viral enzyme that inserts the viral genome into the DNA of the host cell so blocking the retroviral replication.

It is clear that, with different mechanisms, there are two levels in which medications can interrupt the virus spread: the reduction of the virus replication and the healthy cells infection. Accordingly to these observation, the controls u_1 and u_2 denotes all the interventions devoted to the new infection reduction, in the plasma and in the brain respectively, thus emptying the T^*, M^* and M_B^* compartments; at the same time, u_3 for the plasma and u_4 for the brain act to limit the production of new virions, so "starving" the V and V_B compartments.

The model (1) can be rewritten in a compact form after the introduction of the state

$$X = (T \quad T^* \quad M \quad M^* \quad M_B \quad M_B^* \quad V \quad V_B)^T \tag{2}$$

with components x_i, $i = 1, \ldots, 8$, of the control:

$$U = (u_1 \quad u_2 \quad u_3 \quad u_4)^T \tag{3}$$

and of the vector fields

$$f(X) = \begin{pmatrix} \tau - \beta x_7 x_1 - d x_1 \\ \beta x_7 x_1 - \delta x_2 \\ \tau_M + \psi x_5 - \beta_M x_7 x_3 - \varphi x_3 - d_M x_3 \\ \beta_M x_7 x_3 + \psi x_6 - \varphi x_4 - \delta_M x_4 \\ \varphi x_3 - \psi x_5 - \beta_M x_8 x_5 - d_M x_5 \\ \beta_M x_8 x_5 - \psi x_6 + \varphi x_4 - \delta_M x_6 \\ p x_2 + p_M x_4 - c x_7 \\ p_M x_6 - c x_8 \end{pmatrix} \tag{4}$$

$$g(X,U) = \begin{pmatrix} \beta x_1 x_7 u_1 \\ -\beta x_1 x_7 u_1 \\ \beta_M x_3 x_7 u_1 \\ -\beta_M x_3 x_7 u_1 \\ \beta_M x_5 x_8 u_2 \\ -\beta_M x_5 x_8 u_2 \\ -p x_2 u_3 - p_M x_4 u_3 \\ -p_M x_6 u_4 \end{pmatrix} \tag{5}$$

with $g(X, 0) = 0$, thus writing (1) as

$$\dot{X}(t) = f(X) + g(X,U) \tag{6}$$

with given initial conditions $X(t_0)$.

2.2. Existence result

The existence of the solution of the dynamical system (6) may be assessed by using the same arguments as in (Zaman et al., 2008), (Birkhoff & Rota, 1989) and (Iacoviello & Stasio, 2013). In fact, the system (6) may be rewritten as:

$$\dot{X} = A \cdot X + B(X) \tag{7}$$

with:

$$A = \begin{pmatrix} -d & 0 & 0 & 0 & 0 & 0 & 0 & 0 \\ 0 & -\delta & 0 & 0 & 0 & 0 & 0 & 0 \\ 0 & 0 & -\rho_1 & 0 & \psi & 0 & 0 & 0 \\ 0 & 0 & 0 & -\rho_2 & 0 & \psi & 0 & 0 \\ 0 & 0 & \varphi & 0 & -\rho_3 & 0 & 0 & 0 \\ 0 & 0 & 0 & \varphi & 0 & -\rho_4 & 0 & 0 \\ 0 & p(1-u_3) & 0 & p_M(1-u_3) & 0 & 0 & -c & 0 \\ 0 & 0 & 0 & 0 & 0 & p_M(1-u_4) & 0 & -c \end{pmatrix} \tag{8}$$

where the following notations are introduced:

$$\begin{array}{ll} \rho_1 = \varphi + d_M & \rho_2 = \varphi + \delta_M \\ \rho_3 = \psi + d_M & \rho_4 = \psi + \delta_M \end{array} \tag{9}$$

and:

$$B(X) = \begin{pmatrix} \tau - \beta(1-u_1)VT \\ \beta(1-u_1)VT \\ \tau_M - \beta_M(1-u_1)VM \\ \beta_M(1-u_1)VM \\ -\beta_M(1-u_2)V_B M_B \\ \beta_M(1-u_2)V_B M_B \\ 0 \\ 0 \end{pmatrix} \tag{10}$$

From the Holder inequality, it results:

$$|B(X_1) - B(X_2)| \quad \leq \quad C_1 \cdot (|V_1 - V_2| + |T_1 - T_2| + |M_1 - M_2| + \quad |V_{B1} - V_{B2}| + |M_{B1} - M_{B2}|) \tag{11}$$

where X_1 and X_2 denote two different states:

$$X_i = (T_i \quad T_i^* \quad M_i \quad M_i^* \quad M_{iB} \quad M_{iB}^* \quad V_i \quad V_{iB})^T, \qquad i = 1, 2 \tag{12}$$

and the constant C_1 does not depend on the state variables. Therefore, it results, setting $H(X) = A \cdot X + B(X)$:

$$|H(X_1) - H(X_2)| \leq C_2 \cdot |X_1 - X_2| \tag{13}$$

being $C_2 = \max\{C_1, \|A\|\}$. The inequality (13) implies that function H is uniformly Lipschitz continuous. Therefore, considering the limitations in the controls u_i, $i = 1, \ldots, 4$, as well as the positiveness of the state variables, it can be stated the existence of the solution of the system (6).

3. Model analysis

In this section, it will be first analysed the system by determining the disease free equilibrium point and studying its stability characteristics; successively, the expression of the reproduction number will be determined, an important parameter that yields information on the spread of epidemic without the application of any containment measures and which is related to the stability conditions of the dynamics.

3.1. Epidemic free equilibrium condition

To obtain the equilibrium points it has to be solved the system:

$$\dot{X}(t) = 0 \tag{14}$$

The *disease free equilibrium point* is always present in epidemic spread dynamics; it corresponds to the case $T^* = M^* = M_B^* = 0$ (that is with compartments of infected elements void) and with no virions $V = V_B = 0$, that is $x_2 = x_4 = x_6 = x_7 = x_8 = 0$. In absence of control, the values for the other compartments can be obtained solving the reduced system

$$\tau - dx_1^e = 0 \tag{15}$$

$$\tau_M + \psi x_5^e - \varphi x_3^e - d_M x_3^e = 0 \tag{16}$$

$$\varphi x_3^e - \psi x_5^e - d_M x_5^e = 0 \tag{17}$$

One gets

$$x_1^e = \frac{\tau}{d} \tag{18}$$

$$(\varphi + d_M)x_3^e - \psi x_5^e = \tau_M$$

$$\varphi x_3^e - (\psi + d_M)x_5^e = 0$$

thus obtaining:

$$x_3^e = \frac{\tau_M(\psi + d_M)}{\Delta_0} \qquad x_5^e = \frac{\tau_M \varphi}{\Delta_0}$$

with $x_3^e > 0$ and $x_5^e > 0$ since

$$\Delta_0 = (\psi + d_M)(\varphi + d_M) - \psi\varphi = (\psi + \varphi + d_M)d_M > 0 \tag{19}$$

Then, the epidemic free equilibrium point has the full expression

$$P_{DFE} = \left(\frac{\tau}{d} \quad 0 \quad \frac{\tau_M(\psi + d_M)}{\Delta_0} \quad 0 \quad \frac{\tau_M \varphi}{\Delta_0} \quad 0 \quad 0 \quad 0\right)^T \tag{20}$$

clearly with the presence of healthy cells only.

3.2. Partial infected cells

It is worth noting that it is not possible to have equilibrium conditions with a partial presence of infected cells.

- If no virions inside the brain are present, $x_8^e = 0$, from the system (14) it is obtained directly:

$$x_6^e = x_4^e = 0, \qquad x_3^e \cdot x_7^e = 0 \tag{21}$$

For $x_7^e = 0$ P_{DFE} is easily obtained while, if $x_3^e = 0$, no solution is possible, coherently with real biological conditions: in fact $x_3^e = 0$ implies, for the equilibrium computations, both $x_5^e = 0$ and $x_5^e = -\frac{\tau_M}{\psi}$.

- If no virions outside the brain are present, so that $x_7^e = 0$, the point P_{DFE} is deduced immediately once again.
- If no infected macrophages inside the brain are present, $x_6^e = 0$, from the last equation in (1) it is deduced $x_8^e = 0$ and therefore, again, the point P_{DFE} is obtained.
- The same results are easily obtained assuming no infected macrophages outside the brain, $x_4^e = 0$.
- If no infected $CD4 + T$ cells are present, so that $x_2^e = 0$, it follows easily that $x_1^e \cdot x_7^e = 0$, that, being $x_1^e \neq 0$, implies $x_7^e = 0$, yielding again P_{DFE}.

3.3. Stability analysis

The local stability characteristics of the disease free equilibrium condition can be analysed computing the local linearization by means of the Jacobian J evaluated in P_{DFE}:

$$J(P_{DEF}) = \left(\begin{array}{c|ccccccc} -d & 0 & 0 & 0 & 0 & 0 & -\eta_1 & 0 \\ \hline 0 & -\delta & 0 & 0 & 0 & 0 & \eta_1 & 0 \\ 0 & 0 & -\rho_1 & 0 & \psi & 0 & -\eta_2 & 0 \\ 0 & 0 & 0 & -\rho_2 & 0 & \psi & \eta_2 & 0 \\ 0 & 0 & \varphi & 0 & -\rho_3 & 0 & 0 & -\eta_3 \\ 0 & 0 & 0 & \varphi & 0 & -\rho_4 & 0 & \eta_3 \\ 0 & p & 0 & p_M & 0 & 0 & -c & 0 \\ 0 & 0 & 0 & 0 & 0 & p_M & 0 & -c \end{array}\right)$$

Where the following notations are used for sake of compactness:

$$\eta_1 = \beta T_{ef} = \frac{\beta\tau}{d}$$

$$\eta_2 = \beta_M M_{ef} = \frac{\beta_M \tau_M(\psi + d_M)}{\Delta_0} \tag{23}$$

$$\eta_3 = \beta_M M_{Bef} = \frac{\beta_M \tau_M \varphi}{\Delta_0}$$

The real values of the 8 eigenvalues of $J(P_{DEF})$ yield information on the stability of P_{DFE}; besides the eigenvalue $-d$, obviously negative, explicit expressions of the other 7 eigenvalues are not computable.

A different approach, which easily yields sufficient conditions on the allocation of the eigenvalues of matrix (22) makes use of the Gershgorin circles. Based on this result, the eigenvalues of a square matrix of dimension $n \times n$ are contained in the subset of the complex plane constituted by the union of n circles centred in each point of the diagonal and with radius equal to the sum of the modulus of the elements of relating column, without taking the considered diagonal point. The same result holds if each radius is computed by the sum of the modulus of the element of the relating row, again without taking the considered diagonal point. Since all the entries on the diagonal are real and negative, a sufficient condition for having all the eigenvalues with negative real part is that each radius is smaller than the modulus of the diagonal element, so having all the circles confined in the negative half complex plane. The non trivial sufficient conditions obtained by applying the Gershgorin circles column-wise, are, for $i = 2, \ldots, n$

$$p < \delta \tag{24}$$

$$p_M < \delta_M \tag{25}$$

$$2\frac{\beta\tau}{d} + 2\frac{\beta_M \tau_M(\psi + d_M)}{(\psi + d_M)(\varphi + d_M) - \varphi\psi} < c \tag{26}$$

$$2\frac{\beta_M \tau_M \varphi}{(\psi + d_M)(\varphi + d_M) - \varphi\psi} < c \tag{27}$$

The result is intuitive: asymptotic stability is guaranteed if the rate of death of infected cells is greater than that of generation.

3.4. The reproduction number

The virus spread can be measured making use of the *basic reproduction number*, R_0, an indicator of the diffusivity of the virus at the beginning of the infection, in absence of containment measures; it can be evaluated from the mathematical model computing the next generation matrix, (Van Den Driessche, 2017).

According to this approach, from dynamics (6) only the states directly involved by the infection must be considered

$$Z(t) = (\, x_2(t) \quad x_4(t) \quad x_6(t) \quad x_7(t) \quad x_8(t) \,)^T \tag{28}$$

so describing the first infection, and assuming the absence of control. The corresponding dynamical equations are split separating the contagion phase $\mathcal{F}$ and the illness evolution $\mathcal{V}$

$$\dot{Z} = \begin{pmatrix} \dot{X}_2 \\ \dot{X}_4 \\ \dot{X}_6 \\ \dot{X}_7 \\ \dot{X}_8 \end{pmatrix} = \begin{pmatrix} \beta x_1 x_7 \\ \beta_M x_3 x_7 \\ \beta_M x_5 x_8 \\ 0 \\ 0 \end{pmatrix} - \begin{pmatrix} \delta x_2 \\ -\psi x_6 + \varphi x_4 + \delta_M x_4 \\ \psi x_6 - \varphi x_4 + \delta_M x_6 \\ -p x_2 - p_M x_4 + c x_7 \\ -p_M x_6 + c x_8 \end{pmatrix} = \mathcal{F} - \mathcal{V} \tag{29}$$

By linearization in a neighbourhood of the disease free equilibrium point $Z^e = (x_2^e \quad x_4^e \quad x_6^e \quad x_7^e \quad x_8^e)^T$ of the two terms $\mathcal{F}$ and $\mathcal{V}$, one gets.

$$\left.\frac{\partial \mathcal{F}}{\partial Z}\right|_{Z^e} = F = \left(\begin{array}{ccc|cc} 0 & 0 & 0 & \eta_1 & 0 \\ 0 & 0 & 0 & \eta_2 & 0 \\ 0 & 0 & 0 & 0 & \eta_3 \\ \hline 0 & 0 & 0 & 0 & 0 \\ 0 & 0 & 0 & 0 & 0 \end{array}\right) = \begin{pmatrix} 0 & F_{1,2} \\ 0 & 0 \end{pmatrix}$$

And.

$$\left.\frac{\partial \mathcal{V}}{\partial Z}\right|_{Z^e} = G = \left(\begin{array}{ccc|cc} \delta & 0 & 0 & 0 & 0 \\ 0 & \rho_2 & -\psi & 0 & 0 \\ 0 & -\varphi & \rho_4 & 0 & 0 \\ \hline -p & -p_M & 0 & c & 0 \\ 0 & 0 & -p_M & 0 & c \end{array}\right) = \begin{pmatrix} G_{1,1} & 0 \\ G_{2,1} & G_{2,2} \end{pmatrix}$$

Where positions (23) are used once again. The reproduction number is given by the spectral radius of the matrix FG^{-1}, that is, thanks to the structures of the two matrices F and G, by the spectral radius of the matrix $-F_{1,2}G_{2,2}^{-1}G_{2,1}G_{1,1}^{-1}$:

$$-F_{1,2}G_{2,2}^{-1}G_{2,1}G_{1,1}^{-1} = \begin{pmatrix} \eta_1 m_2 & \rho_4 \eta_1 p_M m_1 & \psi \eta_1 p_M m_1 \\ \eta_2 m_2 & \rho_4 \eta_2 p_M m_1 & \psi \eta_2 p_M m_1 \\ 0 & \varphi \eta_3 p_M m_1 & \rho_2 \eta_3 p_M m_1 \end{pmatrix} \tag{32}$$

with

$$m_1 = \frac{1}{c(\rho_2 \rho_4 - \psi \varphi)} \qquad m_2 = \frac{p}{c\delta} \tag{33}$$

It can be easily deduced that one of the eigenvalues of (32) is null; therefore the reproduction number R_0 is given by the largest solution in modulus of the second order equation

$$y^2 - ay + b = 0 \tag{34}$$

with

$$a = \eta_1 m_2 + \rho_4 \eta_2 p_M m_1 + \rho_2 \eta_3 p_M m_1 \tag{35}$$

$$b = \eta_3 p_M m_1 (\eta_1 m_2 \rho_2 + \eta_2 p_M m_1 \rho_2 \rho_4 - \eta_2 p_M m_1 \psi \varphi) \tag{36}$$

4. Optimal control strategy

The introduced controls $u_i(t)$, $i = 1, \ldots, 4$ are defined as the result of pharmacological actions devoted to reduce the proliferation of infected cells by limiting the presence of virions and limiting the virions generation. The mathematical model discussed in Section 3 shows that the presence of just one cell of virions or of infected cells is able of activating the infection; this is due to the macrophages able to go across the brain barrier, also if infected, and to the feeding action of infected cells that improve the number of virions, both inside and outside the brain. These two actions are governed, respectively by the coefficients β, β_M, driving the growth of the infected cells, and by p, p_M, forcing the growth of the virions.

Then, the controls act as reducing factors for the containment, or the full elimination, of the proliferation of $(V, V_B, T^*, M^*, M_B^*)$ cells: a reduction of the infection of T cells, as well as of the macrophages cells M and M_B, along with the limitation of the production of new virions V and V_B from the infected cells.

In (Barker & Vaidya, 2020), the main goal is to study the impact of the virus produced in the brain, both suppressing the viral production outside the brain (and therefore choosing $p = p_M = 0$), and allowing the viral production inside (therefore $p_M > 0$ inside the brain). These controls correspond to a boundary constant action over some inputs, showing that with the application of control inside the brain the influence on the persistence of virus can be significant.

With the model and the controls adopted, it is possible to study all the mutual aspects of interactions for disease containment, being possible 1) to extend the results in (Barker & Vaidya, 2020) allowing a control modulation over time (not only corresponding to no action or maximum efficacy), 2) to introduce a cost in the control application (cost of the drug and physical side effects), 3) to evaluate the advantage of different infected cells reductions, separately or in suitable combinations.

The limitations of the efficacy and availability of each control make the problem more intriguing, requiring suitable choices and timing.

To this aim, optimal control design represents a suitable framework to determine the strategies satisfying the previously chosen requirements; the Pontryagin principle is therefore applied checking the satisfaction of the necessary conditions.

The general approach starts from the definition of the cost index to be minimised, $J(X(t), U(t))$, in which each state and control variables contribute according to their relevance in the desired solution to be computed. Its general expression is given by

$$J(X(t), U(t)) = \int_{t_0}^{t_f} L(X(t), U(t))dt \tag{37}$$

When there are not physical reasons or particular constraints, the general expression $L(t, X(t), U(t))$ in (37) is usually simplified mainly for facilitating the computations and giving a more effective solution. A most adopted approach is represented by a quadratic function

$$L(X(t), U(t)) = X^T(t)Q(t)X(t) + U^T(t)R(t)U(t) \tag{38}$$

with $Q(t) \geq 0$ and $R(t) > 0$.

In this work, the same choice is adopted with further simplifications, taking the weight matrices Q and R diagonal and with no time dependency; this choice is sufficient since the time interval considered is already a small transient time and any further diversification of weights within that short time period seemed not relevant. However, if it were done, the formulas in the sequel do not change but for the time dependency. So,

$$L(X(t), U(t)) = \sum_{i=1}^{8} q_i x_i^2 + \sum_{i=1}^{4} r_i u_i^2 \tag{39}$$

With this general expression it is possible both to minimize the number of infected cells and of virions and, also, to maximize the number of healthy cells (by choosing negative weights for the corresponding weights). In this paper it will be considered the former goal, thus assuming: $q_1 = q_3 = q_5 = 0$.

Before applying the Pontryagin principle and determining the necessary conditions for optimal control, it is possible to state the existence of the optimal control itself by using the arguments in (Fleming & Rishel, 1975):

- The set of controls and state variables is non-empty: this condition is satisfied by the results in (Lukes, 1982).
- The control space is closed and convex: this is due by the box constraints chosen for the control.
- The right hand side of the state system is bounded by a linear function in the state and control: this condition has already been discussed in the previous subsection 2.2.
- The integrand in the cost index is convex with respect to the controls u_i, $i = 1, \ldots, 4$: this is guaranteed by the choice of a positive defined quadratic lagrangian.
- There exists a constant η larger than 1 and two positive constants o_1, o_2 such that:

$$J(u_1, u_2, u_3, u_4) \leq o_2(|u_1|^2 + |u_2|^2 + |u_3|^2 + |u_4|^2) - o_1 \tag{40}$$

This condition is verified once it is considered that the state variables are limited.

Under these arguments, the existence of the optimal control of the considered problem is stated. To determine the necessary optimality conditions it is required the definition of the Hamiltonian:

$$H(X(t),U(t),\lambda(t)) = \sum_{i=1}^{8} q_i x_i^2 + \sum_{i=1}^{4} r_i u_i^2 + \lambda^T(t)(f(X(t)) + g(X(t),U(t)) \tag{41}$$

The costate equations become:

$$\dot{\lambda}_i(t) = -2q_i x_i - \lambda^T(t)\frac{\partial f(X(t)) + g(X(t),U(t)}{\partial x_i} \qquad i = 1,\ldots,8 \tag{42}$$

that is, recalling the notation $X = (T \quad T^* \quad M \quad M^* \quad M_B \quad M_B^* \quad V \quad V_B)^T$:

$$\begin{aligned}
\dot{\lambda}_1(t) &= \lambda_1(t)d1 - (\lambda_2(t) - \lambda_1(t))(1-u_1(t))\beta V(t)\\
\dot{\lambda}_2(t) &= -2q_2T^*(t) + \lambda_2(t)\delta - \lambda_7(t)(1-u_3(t))p\\
\dot{\lambda}_3(t) &= -(\lambda_4(t) - \lambda_3(t))(1-u_1(t))\beta_M V(t) + \lambda_3(t)(\varphi + d_M) - \lambda_5(t)\varphi\\
\dot{\lambda}_4(t) &= -2q_4M^*(t) - \lambda_4(t)(\psi - \varphi - \delta_M) - \lambda_6(t)\varphi - \lambda_7(t)(1-u_3(t))p_M\\
\dot{\lambda}_5(t) &= -\lambda_5(t)(-\psi - d_M) - (\lambda_6(t) - \lambda_5(t))(1-u_2(t))\beta_M V_B(t)\\
\dot{\lambda}_6(t) &= -2q_6M_B^*(t) - \lambda_4(t)\psi - \lambda_6(t)(-\psi - \delta_M) - \lambda_8(t)(1-u_4(t))p_M\\
\dot{\lambda}_7(t) &= -2q_7V(t) - (\lambda_2(t) - \lambda_1(t))\beta T(t) - (\lambda_4(t) - \lambda_3(t))(1-u_1(t))\beta_M M(t)\\
\dot{\lambda}_8(t) &= -2q_8V_B(t) + \lambda_5(t)(1-u_2(t))\beta_M M_B + c\lambda_8(t)
\end{aligned}$$

Since in the present analysis the final state values are assumed not constrained, in equation (42) the final conditions $\lambda_i(t_f) = 0$, $i = 1, \ldots, 8$ must be introduced.

As far as the variables involved in the Lagrangian function, each component of the control vector is assumed nonnegative and bounded by 1; the zero value corresponds to the absence of control, whereas the maximum one is the ideal case of a totally effective therapeutic action which inhibits, where applied, any virus replication. So, bounds of the form $0 \le u_i \le 1$, $i = 1, \ldots, 4$, are introduced.

In a minimization procedure as the one here adopted, it is clear that the quantities to be minimised are the infected and the infective cells, T^*, M^*, M_B^*, V and V^* while the healthy ones, T, M and M_B, must be left unchanged. Then, in the choice of the coefficients q_i, only the ones multiplying the state variables to be minimised must be set greater than zero. For the remaining ones, or the coefficients are set to zero, or, thanks to relative weight of the variables in $L(\bullet)$, they can be set lower than zero, so realising a maximization effect or, in other words, improving the difference between healthy and dangerous cells.

With the general approach described, the Pontryagin principle yields the optimal control as the solution of the inequality:

$$U^o(t) = min(H(X,U,\lambda)), \qquad U \in [0,1] \tag{43}$$

thus yielding

$$u_i^o(t) = min\left\{1, max\left\{\frac{\bar{u}_i(t)}{2r_i}, 0\right\}\right\} \tag{44}$$

where

$$\begin{aligned}
\bar{u}_1(t) &= (\lambda_2(t) - \lambda_1(t)\beta V(t)T(t) + \lambda_4(t) - \lambda_3(t))\beta_M V(t)M(t)\\
\bar{u}_2(t) &= (\lambda_6(t) - \lambda_5(t))\beta_M V_B(t)M_B(t)\\
\bar{u}_3(t) &= \lambda_7(t)(p_M M^*(t) - pT^*(t))\\
\bar{u}_4(t) &= \lambda_8(t)p_M M_B^*(t)
\end{aligned}$$

5. Numerical results

In this section numerical simulations are performed to describe all the previously discussed considerations on the mathematical model (1), and to compute optimal control strategies that correspond to different choices in the pharmacological intervention, comparing them in terms of effectiveness in the infection reduction or eradication along with the evaluation of the optimality of the intensity of the drugs administered.

In all the simulations, the values of the parameters are assumed as in (Barker & Vaidya, 2020), based on experiments with real data, and are here reported in Table 1.

With such parameters, the epidemic free equilibrium point is given by

$$P_{DFE} = \begin{pmatrix} 38700 & 0 & 1.4766 \cdot 10^6 & 0 & 6.3614 \cdot 10^3 & 0 & 0 & 0 \end{pmatrix}^T \tag{45}$$

The Jacobian (22) is:

$$J(P_{DEF}) = \begin{pmatrix} -10^{-2} & 0 & 0 & 0 & 0 & 0 & -1.4 \cdot 10^{-3} & 0 \\ 0 & -1.4 & 0 & 0 & 0 & 0 & 1.4 \cdot 10^{-3} & 0 \\ 0 & 0 & -4 \cdot 10^{-2} & 0 & 8.9 & 0 & -1.3 \cdot 10^{-3} & 0 \\ 0 & 0 & 0 & -0.24 & 0 & 8.9 & 1.3 \cdot 10^{-3} & 0 \\ 0 & 0 & 3.8 \cdot 10^{-2} & 0 & -8.9 & 0 & 0 & -5.5 \cdot 10^{-6} \\ 0 & 0 & 0 & 3.8 \cdot 10^{-2} & 0 & -9.2 & 0 & 5.5 \cdot 10^{-6} \\ 0 & 5 \cdot 10^4 & 0 & 10^3 & 0 & 0 & -23 & 0 \\ 0 & 0 & 0 & 0 & 0 & 10^3 & 0 & -23 \end{pmatrix}$$

whose eigenvalues are

$$\begin{array}{llll} \alpha_1 = -0.0100 & \alpha_2 = -25.8875 & \alpha_3 = -23.0004 & \alpha_4 = 1.4691 \\ \alpha_5 = -0.2429 & \alpha_6 = -0.0018 & \alpha_7 = -9.2394 & \alpha_8 = -9.0359 \end{array}$$

Therefore the disease free equilibrium point is unstable as could be hypothesized directly checking the conditions (24)–(27), being the first two not verified. The instability of the disease free equilibrium point is connected with the basic reproduction number R_0, that can be determined by solving (34), once a and b are calculated resulting equal to 2.34 and $7.07 \cdot 10^{-5}$ respectively. In this case $R_0 = 2.26 > 1$, meaning that without control actions the spread increases.

The framework considered in this paper to face the infection is the optimal control; for the initial conditions the values adopted are: $T_i = 38700$, $M_i = 1463000$, $M_{Bi} = 200$; for the infected cells null values: $T_i^* = M^* = M_{Bi}^* = 0$, with $V_i = 0$ and $V_{Bi} = 100$, therefore, assuming that the infection is originated by the presence of virions V_b only.

As far as the lagrangian (39) is concerned, the choice is to minimize the infected cells T^*, M^*, M_B^* and the virions, both outside and inside the brain V and V_B respectively, without aiming at increasing the number of healthy cells, $q_1 = q_3 = q_5 = 0$.

As a possible choice of the weights q_2, q_4, q_6, q_7, q_8 and r_i, $i = 1, \ldots, 4$, it is proposed to assume them in order to have the terms of the cost index comparable in the control time interval, considering the order of magnitude of the values of the states in a simulation up to 100 days in absence of control and the square applied in the cost index, thus having:

$$q_2 = q_4 = q_6 = q_8 = 10^{-9} \qquad q_7 = 10^{-12} \tag{46}$$

and, for the weights of the control

$$r_i = 10^{-2} \quad i = 1, 2, 3, 4 \tag{47}$$

To appreciate the effects of the introduction of optimal controls, two situations are simulated, comparing what would happen if no actions were applied for the entire control period of 60 days, and if the optimal control is applied starting at the 16th day (indicated in the following as *simulation 1*) and if the optimal control is applied from the 20th day (indicated in the following as *simulation 2*). The first choice, starting from the 16th day, corresponds to the beginning of the sensible increase of the number of virions V cells; the second, from the 20th day, corresponds to starting the action at the peak of the number of virions V.

The optimal controls u_i^o, $i = 1, \ldots, 4$ are shown in Fig. 2; more precisely, in Fig. 2 panel *a* the controls u_1^o and u_3^o acting outside the brain are shown in the two simulated cases (control action starting at day 16 and starting at day 20). It can be noted that, if the controls are applied only starting at day 20, the effort to be applied, both for u_1^o and u_3^o, is stronger with respect to an earlier application. In particular u_1^o in simulation 1 has an almost constant value around 0.4, whereas it is decreasing from a

Table 1
Numerical values of the model parameters.

Parameter	Value	Parameter	Value
τ	387 $[\mu l^{-1} d^{-1}]$	τ_M	2743.55 $[\mu l^{-1} d^{-1}]$
β	$3.583 \cdot 10^{-8}$ $[\mu l\, d^{-1}]$	β_M	$8.65 \cdot 10^{-10}$ $[\mu l\, d^{-1}]$
d	0.01 $[d^{-1}]$	d_M	0.00185 $[d^{-1}]$
δ	1.4551 $[d^{-1}]$	δ_M	0.2060 $[d^{-1}]$
φ	0.03876 $[d^{-1}]$	ψ	8.995 $[d^{-1}]$
p	50000 $[d^{-1}]$	p_M	1000 $[d^{-1}]$
c	23 $[d^{-1}]$		

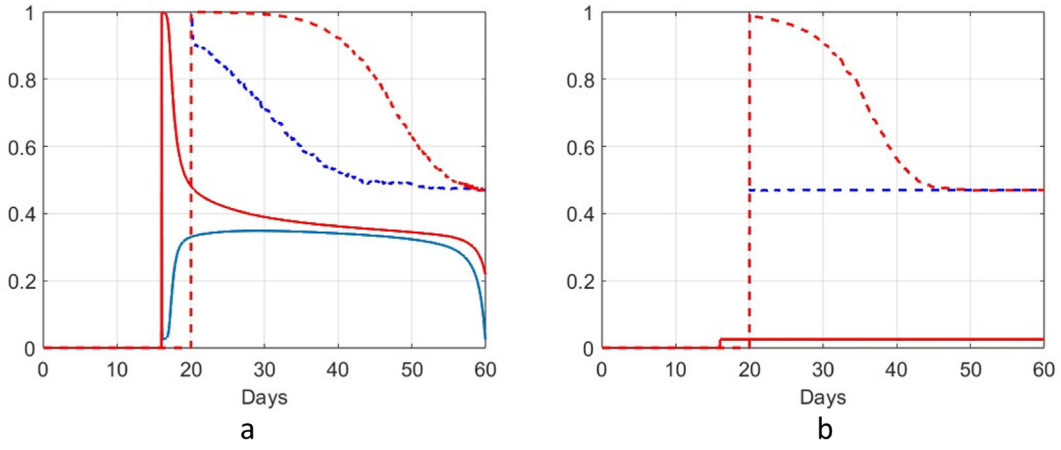

Fig. 2. Evolution of the optimal controls; a) optimal control u_1^o (blu curve) and u_3^o (red curve) when all the actions are applied at day 16 from the beginning of the infection (continuous lines) or at day 20 (dotted lines); b) optimal control u_2^o (blu curve) and u_4^o (red curve) when all the actions are applied at day 16 from the beginning of the infection (continuous lines) or at day 20 (dotted lines).

value of about 0.9 reaching the value of 0.5. Analogously, also u_3^o, in the two cases, reaches the same values, with larger values in simulation 2. In Fig. 2 panel b the controls u_2^o and u_4^o are shown for the two simulations; it can be noted a stronger difference in the values in the two simulations with almost constant values in simulation 1 and for u_2^o for simulation 2. In both cases it can be noted that the controls u_3^o and u_4^o required to minimize the cost index must be stronger than u_1^o and u_2^o, thus suggesting the importance of limiting the feeding actions of $T*$, $M*$ and M_b^* on V and V_b.

Figs. 3–6 show the behaviours of the 8 state variables with the evident advantages of early action (simulation 1); also the introduction of optimal control starting at day 20 provides advantages in a lower number of infected cells, limiting the decrease of the number of healthy cells. In all the evolutions, in particular the ones of $T*$, V and V_b, the effects of the controls avoid to reach the highest values in simulation 1, and allow to reduce rapidly the high values of infected cells and virions in simulation 2.

These effects can be appreciated in Fig. 7 and 9 where the blue lines represent the consequences of the application of the optimal control starting at day 16, and 20, respectively, considering the total healthy cells $T + M + M_b$ (panel a) and infected cells $T^* + M^* + M_b^*$ (panel b). In both cases, and mostly for simulation 1, the benefits of the control actions are evident decreasing the infection effects. To stress the role of the controls inside and outside the brain, two further optimization problems are studied; one assuming in the model, and consequently in the optimal control problem, only the optimal actions inside the brain, thus obtaining new u_2^o and u_4^o, and the other, solving an optimal control problem in which only u_1^o and u_3^o are found, assuming equal to zero u_2 and u_4. It can be noted in Figs. 7 and 9 that in absence of the controls u_1^o and u_3^o the two

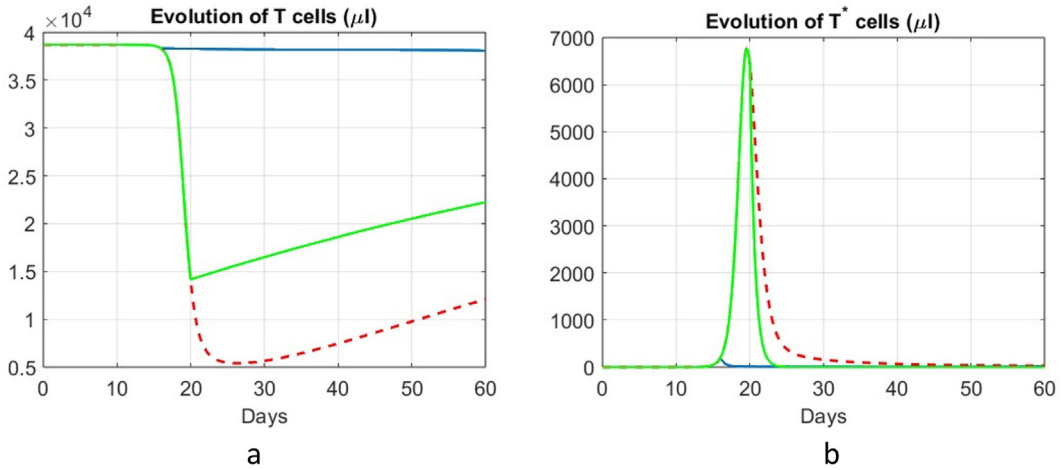

Fig. 3. Evolution of the concentration of the T (a) and $T*$ cells (b) in three conditions: i) no control action applied (red dotted line), ii) assuming no control action up to day 20 and successively with the application of the corresponding optimal controls of Fig. 2 (green line), iii) assuming no control action up to day 16 and successively the application of the corresponding optimal controls of Fig. 2 (blue lines).

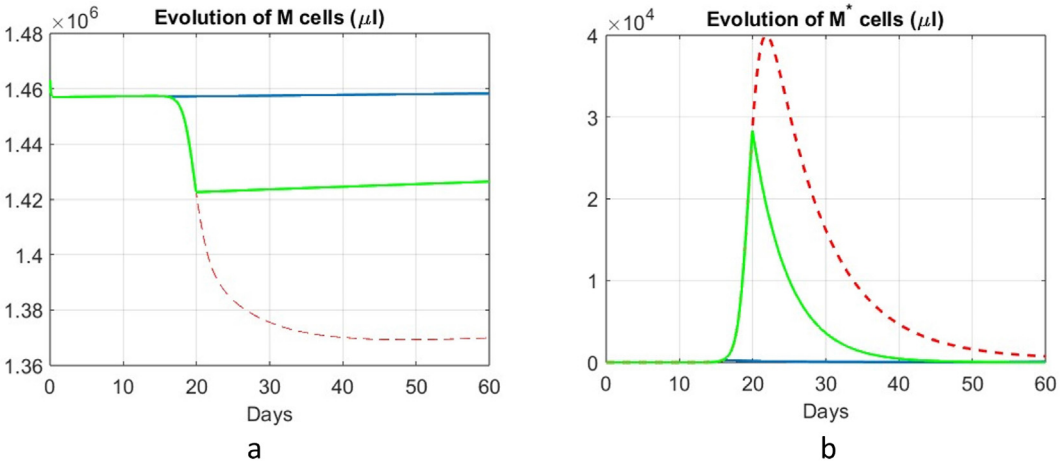

Fig. 4. Evolution of the concentration of the M (a) and M* cells (b) in three conditions: i) no control action applied (red dotted line), ii) assuming no control action up to day 20 and successively with the application of the corresponding optimal controls of Fig. 2 (green line), iii) assuming no control action up to day 16 and successively the application of the corresponding optimal controls of Fig. 2 (blue line).

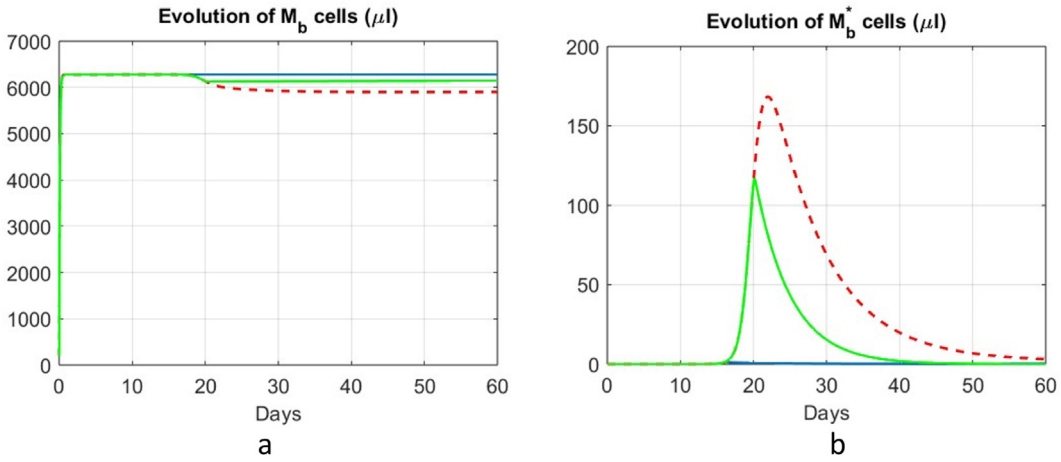

Fig. 5. Evolution of the concentration of the M_b (a) and M_b^* cells (b) in three conditions: i) no control action applied (red dotted line), ii) assuming no control action up to day 20 and successively with the application of the corresponding optimal controls of Fig. 2 (green line), iii) assuming no control action up to day 16 and successively the application of the corresponding optimal controls of Fig. 2 (blue line).

actions u_2^o and u_4^o do not provide a sensible reduction of the infection, whereas the u_1^o and u_3^o do yield advantages in facing the infection, even alone.

In Fig. 8, panel a, it can be noted that the absence of control u_2^o and u_4^o does not basically change the required effort for u_1^o and u_3^o with respect to the original simulation 1, whereas the case in which it is assumed $u_1 = u_3 = 0$ the optimal controls u_2^o and u_4^o try to face the infection with values significantly higher with respect to the application of the control of simulation 1.

In Fig. 10 panel a the optimal controls u_1^o and u_3^o (continuous lines blue and red) of simulation 2 are shown along with the same controls obtained solving the optimization problem with $u_2^o = u_4^o$ (dotted blue and red lines respectively). Analogously, in panel b the optimal controls u_2^o and u_4^o of simulation 2 are shown along with the same control obtained solving the optimization problem with $u_1^o = u_3^o$. In both cases it can be noted that the obtained dotted controls have lower values than the corresponding ones of simulations 1 and 2. The reason is that when applying the controls starting at day 20, that is when the number of infected cells is already decreasing, the best strategy to minimize the chosen cost index (being the sum of the square of infected cells plus the square of the controls) is to apply a lower level of controls.

Finally, in Fig. 11 the effects of simulation 1 (panel a) and simulation 2 (panel b) are shown on the total number of virions $V + V_b$ and compared with the absence of controls, along with the application of the control obtained solving the optimal control problem with $u_1 = u_3 = 0$ and the problem with $u_2 = u_4 = 0$. The predominant role of the controls outside the brain, u_1^o and u_3^o, is evident also on the total number of virions, both for simulations 1 and 2. This is comforting, since, up to now, most of the more common ART therapies have limited capabilities to cross the blood brain barrier. One of the goal of recent research is

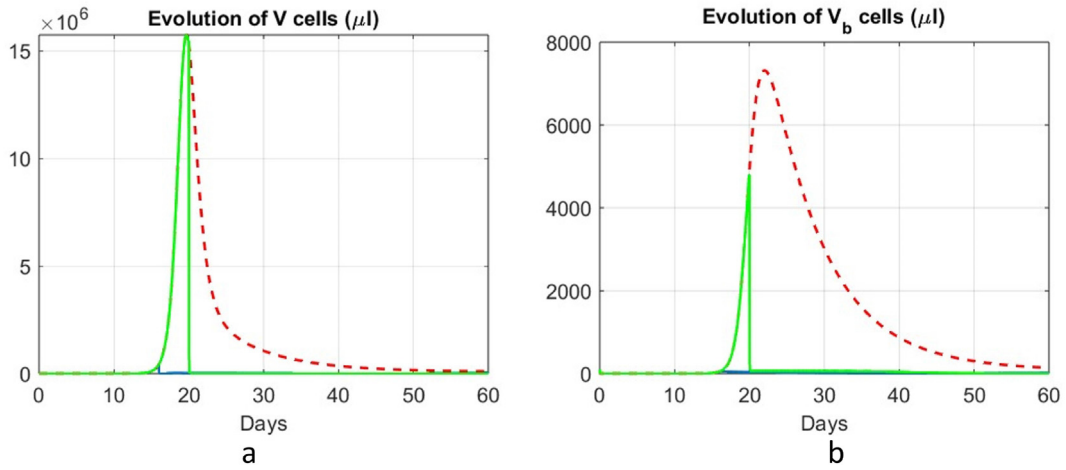

Fig. 6. Evolution of the concentration of the V (a) and V_b cells (b) in three conditions: i) no control action applied (red dotted line), ii) assuming no control action up to day 20 and successively with the application of the corresponding optimal controls of Fig. 2 (green line), iii) assuming no control action up to day 16 and successively the application of the corresponding optimal controls of Fig. 2 (blue line).

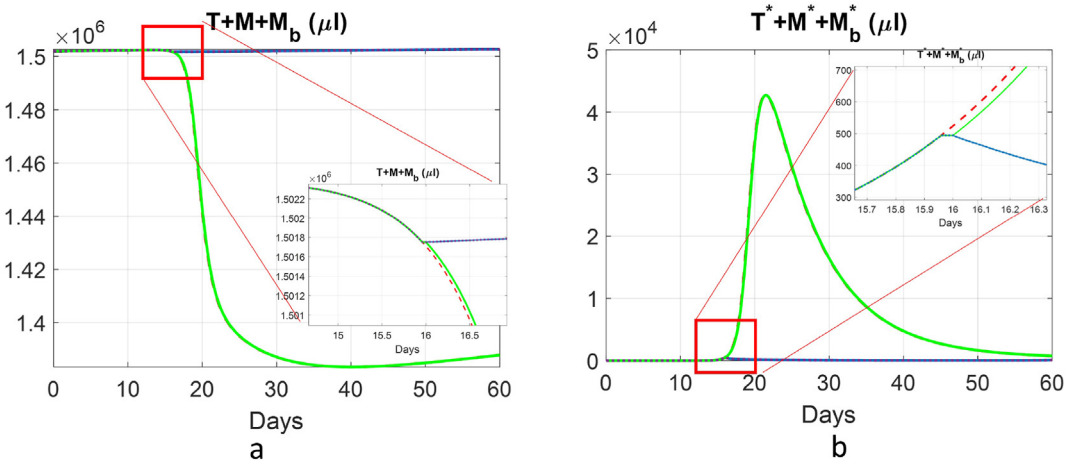

Fig. 7. Evolution of the concentration of the healthy cells $T + M + M_b$ (panel a) and of the infected cells $T^* + M^* + M_b^*$ (panel b) when all the optimal controls starting at day 16 of Fig. 2 are applied (blue solid line), when only controls u_2 and u_4 are used (green line), when only controls u_1 and u_3 are used (dotted line), and without any action (red line).

to provide drugs based on nanoparticles with acceptable biocompatibility with red blood cells and macrophages able to penetrate the BBB; in (Gong et al., 2020), in particular, it is assessed the 50% ability of penetration of PLGA-based EVG nanoparticles in the microglia, important central nervous system HIV-1 reservoir. Nowadays, recent studies, (Mathews et al., 2019), (Anesten et al., 2021) refer to in vitro research and on mice showing promising developments with reference to the possibility of obtaining therapies capable of penetrating the brain and limiting the infection.

6. Conclusions and future developments

The macrophages are the cells able to cross the blood brain barrier from outside to inside the brain and vice versa. HIV can fool these cells that can contribute to the increase of the number of virions. This mechanism makes the brain and other organs a sort of reservoir of HIV thus making difficult to interrupt their proliferation. The description of this phenomenon is herein based on a model already experimentally validated on real data; one basic assumption regards the non inclusion of the cell growth rate, that regards the immature macrophages infected and able to cross the brain barrier. Nevertheless, the simplification does not affect the overall modeling that seems to adequately get the cell dynamics. The control actions introduced, following the possible medical intervention available, discussed in Subsection 2.1, aim at interrupting the infection of healthy cells and the proliferation of virions, outside and inside the brain. In all the analysis it is evident the deeper influence of the control outside the brain with respect to the one inside; this is comforting, at least referring to the most recent available

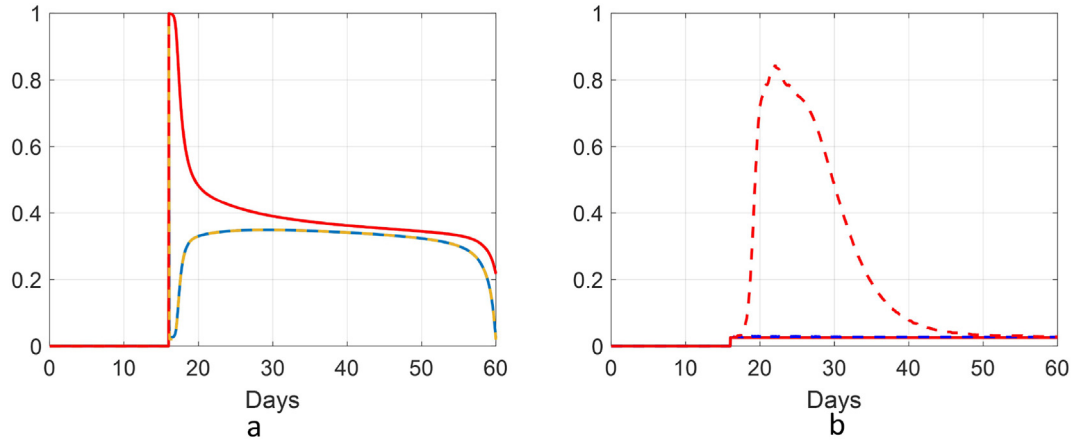

Fig. 8. Evolution of the control actions u_1^o (blu line)and u_3^o (red line) (panel a) and u_2^o (blue line) and u_4^o (red line) (panel b) when all the optimal controls starting at day 16 (solid line), when only controls u_1 and u_3 are used (dotted yellow and red lines respectively) keeping $u_2 = u_4 = 0$, when only controls u_2 and u_4 are used (dotted yellow and red lines respectively), keeping $u_1 = u_3 = 0$.

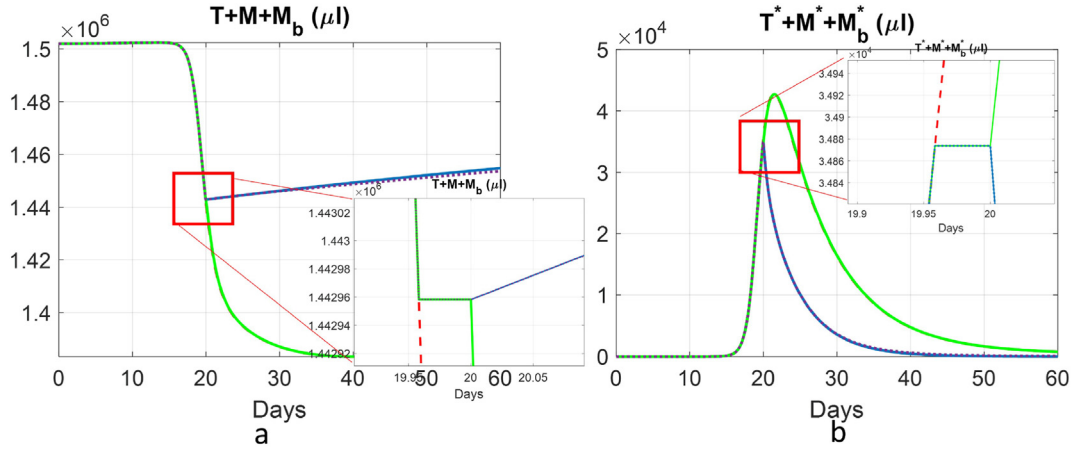

Fig. 9. Evolution of the concentration of the healthy cells $T + M + M_b$ (panel a) and of the infected cells $T^* + M^* + M_b^*$ (panel b) when all the optimal controls starting at day 20 of Fig. 2 are applied (blue solid line), when only controls u_2 and u_4 are used (green line), when only controls u_1 and u_3 are used (dotted line), and without any action (red line).

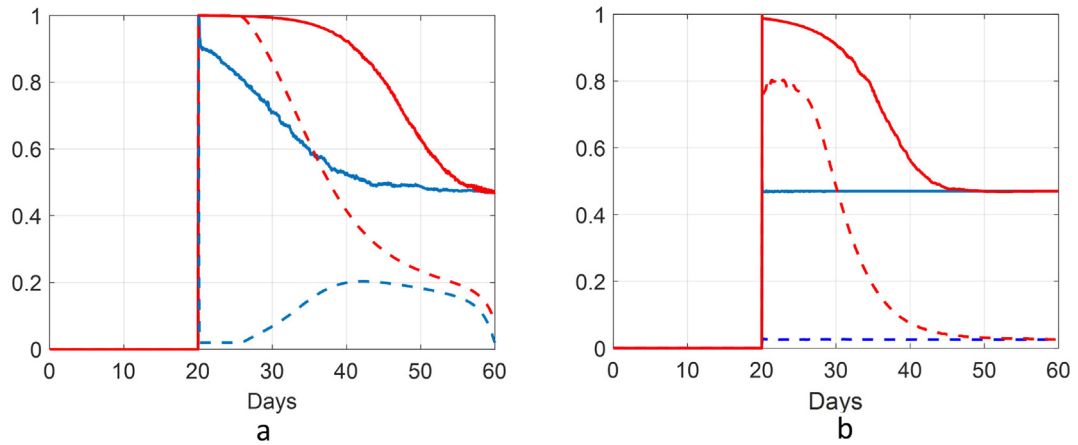

Fig. 10. Evolution of the control actions u_1^o (blu line)and u_3^o (red line) (panel a) and u_2^o (blue line) and u_4^o (red line) (panel b) when all the optimal controls starting at day 20 (solid line) are applied, when only controls u_1^o and u_3^o are used (dotted line) keeping $u_2 = u_4 = 0$, when only controls u_2^o and u_4^o are used (dotted line), keeping $u_1 = u_3 = 0$.

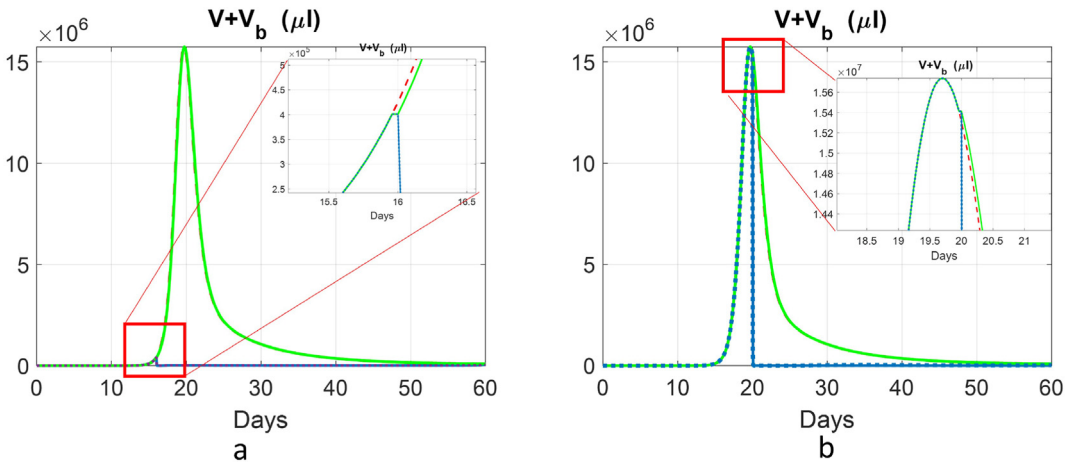

Fig. 11. Evolution of the concentration of the virion cells $V + Vb$ when, in panel a, the control action start at day 16 and when, panel b, it starts at day 20 (blue solid line), when only controls u_2 and u_4 are used (green line), when only controls u_1 and u_3 are used (dotted line), and without any action (red line).

medications. Moreover, it can be stressed the importance of a combination of early treatments, both inside and outside the brain. Ongoing work aims at studying relations among brain and other virus reservoir and the most efficient way of medical treatment.

Conflict of interest

The authors P. Di Giamberardino, D. Iacoviello and M. Zubair declare that there are no conflict of interest concerning the paper "Optimal therapy for HIV infection containment and virions inhibition".

CRediT authorship contribution statement

Paolo Di Giamberardino: Conceptualization, Data curation, Formal analysis, Funding acquisition, Investigation, Methodology, Project administration, Resources, Software, Supervision, Validation, Visualization, Writing – original draft, Writing – review & editing. **Daniela Iacoviello:** Conceptualization, Data curation, Formal analysis, Funding acquisition, Investigation, Methodology, Project administration, Resources, Software, Supervision, Validation, Visualization, Writing – original draft, Writing – review & editing. **Muhammad Zubair:** Writing – review & editing.

References

Agosto, L. M., Zhong, P., Munro, J., & Mothes, W. (2014). Highly active antiretroviral therapies are effective against HIV-1 cell-to-cell transmission. *PLOS Pathogenes, 10*(2), 1–12.
Ahemd, S., Rahman, S., & Kamrujjaman, M. (2021). Optimal treatment strategy to control acute HIV infection. *Infectious Disease Modelling, 6*, 1202–1219.
Anesten, B., Zetterberg, H., Nilsson, S., Brew, B., Fuchs, D., Price, R., Gisslen, M., & Yilmaz, A. (2021). Effect of antiretroviral treatment on blood-brain barrier integrity in HIV-1 infection. *BMC Neurology, 21*.
Astorga-Gamaza, A., & Buzon, M. J. (2021). The active human immunodeficiency virus reservoir during antiretroviral therapy: Emerging players in viral persistence. *Current Opinion in HIV and AIDS, 16*(4), 193–199.
Barker, C. T., & Vaidya, N. K. (2020). Modeling HIV-1 infection in the brain. *PLOS Computational Biosciences*, 1–18.
Birkhoff, G., & Rota, G. C. C. (1989). *Ordinary differential equations* (4th ed.). New York: John Wiley & Sons.
Busman-Sahay, K., Starke, C. E., Nekorchuk, M. D., & Estes, J. D. (2021). Eliminating HIV reservoirs for a cure: The issue is in the tissue. *Current Opinion in HIV and AIDS, 16*(4), 200–208.
Chen, J., Zhou, T., Zhang, Y., Luo, S., Chen, H., Chen, D., Li, C., & Li, W. (2022). The reservoir of latent HIV. *Frontiers in Cellular and Infection Microbiology, 1–15*.
Clifford, D. B., & Ances, B. M. (2013). HIV-associated neurocognitive disorder (HAND). *Lancet Infectious disease, 13*(11), 976–986.
Deeks, S. D., Overbaugh, J., Phillips, A., & Buchbinder, S. (2015). HIV infection. *Nature, 1*, 1–22.
Di Gamberardino, P., & Iacoviello, D. (2018a). LQ control design for the containment of the HIV/AIDS diffusion. *Control Engineering Practice, 77*, 162–173.
Di Gamberardino, P., & Iacoviello, D. (2018b). HIV infection control: A constructive algorithm for a state-based switching control. *International Journal of Control, Automation and Systems, 16*(3), 1469–1473.
Di Gamberardino, P., & Iacoviello, D. (2020). Epidemic modeling and control of HIV/AIDS dynamics in populations under external interactions: A worldwide challenge. *Control Applications for Biomedical Engineering Systems*.
Di Giamberardino, P., Compagnucci, L., De Giorgi, C., & Iacoviello, D. (2019). Modeling the effects of prevention and early diagnosis on HIV/AIDS infection diffusion. *IEEE Transactions on Systems, Man, and Cybernetics: Systems, 49*(10), 2119–2130.
Di Giamberardino, P., & Iacoviello, D. (2023). Early estimation of the number of hidden HIV infected subjects: An extended Kalman filter approach. *Infectious Disease Modelling, 8*(2), 341–355.
Dupont, M., & Sattentau, Q. J. (2020). Macrophages cell-cekk interactions promoting HIV -1 infection. *Viruses, 12*, 1–17.
Eggleton, J. S., & Nagalli, S. (2023). Highly active antiretroviral therapy (HAART). In *StatPearls [Internet]*. Treasure Island (FL): StatPearls Publishing.
Fleming, W. H., & Rishel, R. W. (1975). *Deterministic and stochastic optimal control*. New York: Springer Verlag.

Gong, Y., Zhi, K., Naghesh, P., Sinha, N., Chowdhury, P., Chen, H., Gorantla, S., Yallapu, M., & Kumar, S. (2020). An elvitegravir nanoformulation crosses the blood–brain barrier and suppresses HIV-1 replication in microglia. *Viruses, 564*.
Huang, Y., Zhang, C., Wu, J., & Lou, J. (2017). Modelling the HIV persistence through the network of lymphocyte recirculation in vivo. *Infectious Disease Modeling, 2*, 90–99.
Iacoviello, D., & Stasio, N. (2013). Optimal control for SIRC epidemic outbreak. *Computer Methods and Programs in Biomedicine, 110*, 333–342.
Kruize, Z., & Kootstra, N. A. (2019). The role of macrophages in HIV-1 persistence and pahogenesis. *Frontiers in Microbiology, 10*, 1–17.
Kumar, A., Abbas, W., & Herbein, G. (2014). HIV-1 latency in monocytes/macrophages. *Viruses, 6*(4), 1837–1860.
Levy, J. (1995). HIV and the pathogenesis of AIDS. *Science, 267*.
Lukes, D. L. (1982). Differential equations: Classical to controlled. In *Mathematics in science and engineering* (Vol. 162)New York: Academic Press.
Lutgen, V., Narasipura, S., Barbian, H., Richards, M., Wallace, J., Razmpour, R., Buzhdygan, T., Ramirez, S., Prevedel, L., Eugenin, E., & Harthi, L. (2020). HIV infects astrocytes in vivo and egresses from the brain to the periphery. *PLoS Pathogens, 1–32*.
Mathews, S., Branch-Woods, A., Katano, I., Makarov, E., Thomas, M. B., Gendelman, H. E., Poluektova, L. Y., Ito, M., & Gorantla, S. (2019). Human Interleukin-34 facilitates microglia-like cell differentiation and persistent HIV-1 infection in humanized mice. *Molecular Neurodegeneration, 14*.
Montessori, V., Press, N., Harris, M., Akagi, L., & Montaner, J. S. G. (2004). Adverse effects of antiretroviral therapy for HIV infection. *Canadian Medical Association Journal, 170*(2), 229–238.
Osborne, O., Peyravian, N., Nair, M., Dauneri, S., & Toborek, M. (2020). The paradox of HIV-Blood-Brain Barrier Penetrance and Antiretroviral drug delivery deficiency. *Trends in Neurosciences, 43*(94), 221–240.
Prinz, M., & Priller, J. (2014). Microglia and brain macrophages in the molecular age: From origin to neuropsychiatric disease. *Nature Reviews Neuroscience, 15*(5), 300–312.
Thapa, S., & Shrestha, U. (2023). Immune reconstitution inflammatory syndrome. In *StatPearls [Internet]*. Treasure Island (FL): StatPearls Publishing.
Van Den Driessche, P. (2017). Reproduction numbers of infectious disease models. *Infectious Disease Modelling, 2*(3), 288–303.
WHO. https://www.who.int/news-room/fact-sheets/detail/hiv-aids.
Zaman, G., Kang, Y. H., & Jung, I. H. (2008). Stability analysis and optimal vaccination of an SIR epidemic model. *Biosystems, 93*, 240–249.
Zephyr, J., Kurt Yilmaz, N., & Schiffer, C. A. (2021). Viral proteases: Structure, mechanism and inhibition. *Enzymes, 50*, 301–333.